Journal of Applied Electrochemistry **31**: 591–598, 2001.

Comparative study of the effect of oxygen and oxygen/ozone mixtures on the electrochemical behaviour of different metals

M.R. VIERA, M. FERNANDEZ LORENZO de MELE* and H.A. VIDELA
INIFTA, Department of Chemistry, Faculty of Pure Sciences, University of La Plata, C.C. 16, Suc. 4, 1900, La Plata, Argentina
*(*author for correspondence)*

Received 1 September 2000; accepted in revised form 12 December 2000

Key words: anodic films, carbon steel, copper alloys, passive films, stainless steel, titanium

Abstract

The effect of dissolved ozone on the electrochemical behaviour of heat exchanger structural materials (carbon steel, stainless steel, copper, 70:30 copper–nickel, aluminium brass and titanium grade 1) was studied to evaluate the possibility of using ozone as sole biocide in cooling water treatment. With this purpose, voltammetric and open circuit potential (OCP) against time measurements at different ozone concentrations between 0.1 and 1.2 ppm were made. Results show different electrochemical responses according to the metal characteristics and the solution composition. First, the passivity of titanium and stainless steel was not affected by ozone. A linear OCP against log time relationship was found for titanium, suggesting the growth of a barrier film in both O_2 and O_2/O_3 solutions. Mild steel does not passivate in synthetic cooling water either with O_2 or O_2/O_3 in the solution. In the presence of ozone the breakdown of passivity is facilitated and makes the repassivation difficult. Ozone enhances the dissolution of Cu_2O and the formation of Cu(II) species leading to less protective films. Both processes are strongly influenced by the pH. Finally, the dissolution of aluminium brass is higher than that of copper or copper–nickel.

1. Introduction

Biocorrosion and biofouling have become a major problem in cooling systems because of recent trends in water treatment where slightly alkaline pH values and other biocides than chlorine are used [1]. Cooling water treatment strategies need environmentally safe biocides which must be compatible with system operation and effective to reduce bacterial contamination [2].

In recent years ozone has been recommended as sole biocide for cooling water because of its potential capacity to control not only microbiological fouling but also scaling and corrosion [3–5]. However, results showing that ozone could accelerate metal corrosion have also been reported [5, 6].

Taking into account environmental concerns, the use of ozone presents several advantages with respect to other biocides: (i) minimal on-site inventory: concerns about storage and handling of biocides are minimized since ozone is generated *in situ*; (ii) no-toxicant discharge: its rapid decomposition minimizes down-stream toxicity risks; (iii) potential for water conservation: numerous case histories about the good performance of ozone in 'zero discharge' cooling tower applications have been reported [7]. Ozone decomposition also gives oxygen and thus induces the oxygenation of the discharge water.

Ozone has been effective for killing planktonic cells, but its biocidal efficacy on sessile cells within biofilms is low [8]. Ozone biocidal activity is based on its high oxidizing power (2.07 V vs NHE). Such an oxidizing power could accelerate the metal dissolution. Thus, the goal of this work is to study the effect of ozone on the electrochemical behaviour of heat exchanger constructional materials (carbon steel, stainless steel, copper alloys and titanium) to evaluate the possibility of using this biocide for cooling water treatment. With this aim, the effect of ozone on the electrochemical behaviour of different metals and alloys in synthetic cooling water (SCW) was assayed. Potentiodynamic polarization measurements and open circuit potential (OCP) against time evolution tests in the presence of different ozone concentrations were performed.

2. Experimental methods

2.1. *Ozone generation*

Ozone was generated by corona discharge from pure oxygen. The experimental set-up consisted of a purification system for filtering oxygen gas and eliminating moisture, and the ozone generator itself (Figure 1(a) and (b)). Different levels of dissolved

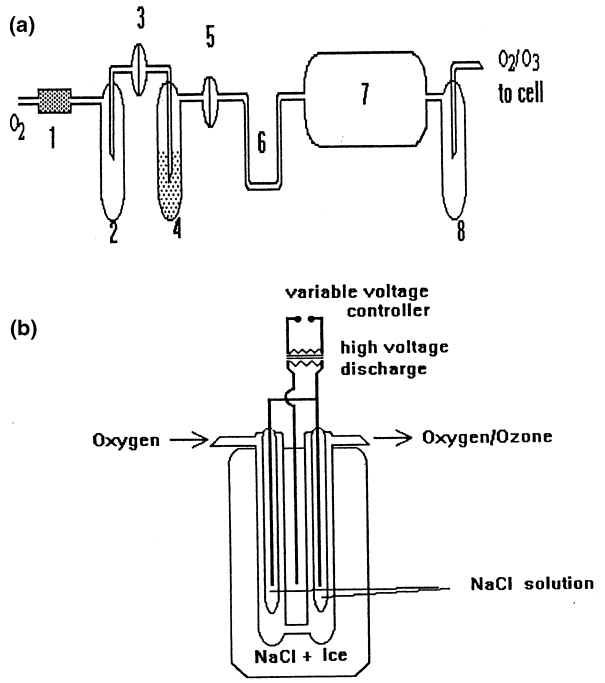

Fig. 1. Schematic diagram of the ozone generator system. (a) Gas purification system and ozone generator; (b) detailed scheme of the ozone generator by corona discharge. Key: (1) glass wool filter, (2) trap, (3 and 5) fritted glass, (4) trap with sulfuric acid, (6) glass spiral, (7) ozone generator and (8) trap.

ozone were obtained by fixing the voltage input at different values, by means of a variable-voltage controller. Ice was added to the NaCl solution in the ozone generator to remove the heat evolved during ozone production.

Dissolved ozone solutions, within the 0.1 to 1.2 ppm concentration range, were obtained by bubbling different oxygen/ozone mixtures in SCW contained in a glass cell. Dissolved ozone concentrations were measured using the indigo trisulfonate method [9].

2.2. *Electrochemical experiments*

Metal specimens used for the electrochemical experiments were: SAE 1020 type carbon steel, AISI 304 type stainless steel (SS), pure copper, 70:30 copper–nickel, aluminium brass and titanium grade 1. Platinum was used as reference material. The chemical composition of these metals is shown in Tables 1 and 2.

Table 2. Chemical composition of copper alloys

Element/%	Cu	Ni	Zn	Al	As	Fe
70:30 Copper–nickel	67	31.9	–	–	–	1.1
Aluminiun brass	77–78	–	19–20	2.4–2.6	0.02	–

The samples were mounted in an epoxy resin, leaving exposed areas of 0.385 cm^2 for carbon steel, 0.320 cm^2 for SS, 0.400 cm^2 for 70:30 copper–nickel, 0.196 cm^2 for pure copper, 0.320 cm^2 for titanium and 0.345 cm^2 for aluminium brass. Metal specimens were wet ground with different grits of silicon metallurgical paper (240, 400 and 500) and finally with alumina paste (1 μm grain size). After polishing, samples were cleaned and degreased with acetone and finally rinsed with distilled water.

The composition of the SCW used as electrolyte in the electrochemical experiments is shown in Table 3.

Electrochemical experiments were carried out in a conventional double-wall glass cell. A platinum electrode was used as counterelectrode and a saturated calomel electrode (SCE) as a reference electrode to which potentials in the text are referred.

Voltamperometric experiments were made at a scan rate of 0.001 V s^{-1} or 0.020 V s^{-1} within the potential range of −1.0 V and 0.5 V vs SCE. OCP and redox potential vs time measurements were also made.

3. Results

The redox potential of a Pt electrode in SCW saturated with O_2 or O_2/O_3 at two ozone concentrations is shown in Figure 2. The potential reached a stable value after a few minutes. It can be seen that the higher the oxidizing power of the solution the higher its potential value.

The evolution of OCP for stainless steel and titanium is shown in Figure 3. When the SCW was saturated with oxygen the potential increased up to a quite stable value for both metals. In the presence of ozone (at very low ozone/oxygen ratios) a relevant change in the OCP behaviour occurred: an initial OCP decrease to a minimum value, was observed. This potential decrease was more noticeable in the case of stainless steel.

Table 1. Chemical composition of stainless steel, carbon steel and titanium

Element/%	Fe	Ti	Ni	C	Si	Cr	Mo	Mn	O	N	H
AISI 304 Stainless steel	balance	–	10.60	0.08	0.31		0.48	0.55	–	–	–
SAE 1020 Carbon steel	balance	–	–	0.1	0.05		–	0.45	–	–	–
Ti Grade 1	max 0.20	balance	–	max 0.08	–		–	–	~0.08	max 0.03	max 0.013

Table 3. Composition of SCW (pH 8.0–8.5)

Ion	Concentration /ppm
Ca^{2+}	25
Na^{+}	40
Mg^{2+}	14
Cl^{-}	105
SO_4^{2-}	53

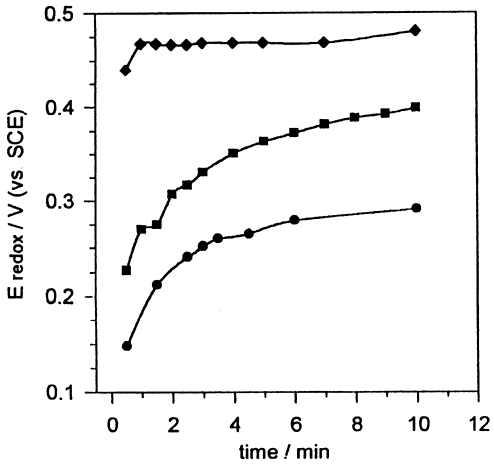

Fig. 2. Redox potential against time plot measured with a Pt electrode immersed in SCW saturated with: (●) O_2; (■) O_2/O_3, $[O_3] = 0.48$ ppm; (◆) $[O_3] = 1$ ppm.

Thereafter, the potential increased, and for both metals, the higher the ozone concentration, the higher the final OCP.

The polarization curves for stainless steel and titanium showed a broad passive potential region up to 0.5 V which was not disturbed by ozone (Figure 4). However, the initial cathodic currents showed significant differences when ozone was present. Under these conditions, higher current values were recorded for stainless steel and lower currents for titanium.

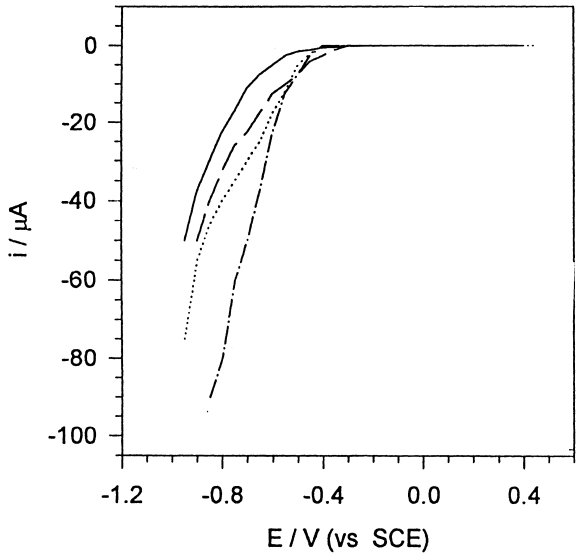

Fig. 4. Voltammograms for SS and Ti made at 0.001 V s^{-1} in SCW saturated with O_2 or O_2/O_3 mixture. Key: (·····) SS/O_2; (— · —) SS/O_3; (——) Ti/O_3; (—) Ti/O_2.

The OCP against time evolution of carbon steel in the presence of oxygen or ozone showed a shift in the active direction to reach a fairly stable value (Figure 5). The final potential values were more anodic at higher ozone concentrations. Localized corrosion was verified by visual and microscopic inspection of the surface of these electrodes after each experiment. The polarization curves (Figure 6) showed a breakdown of passivity for carbon steel in SCW saturated with oxygen at −0.01 V. Both, the breakdown potential (E_b) and the repassivation potential (E_r) were more cathodic in the presence of ozone.

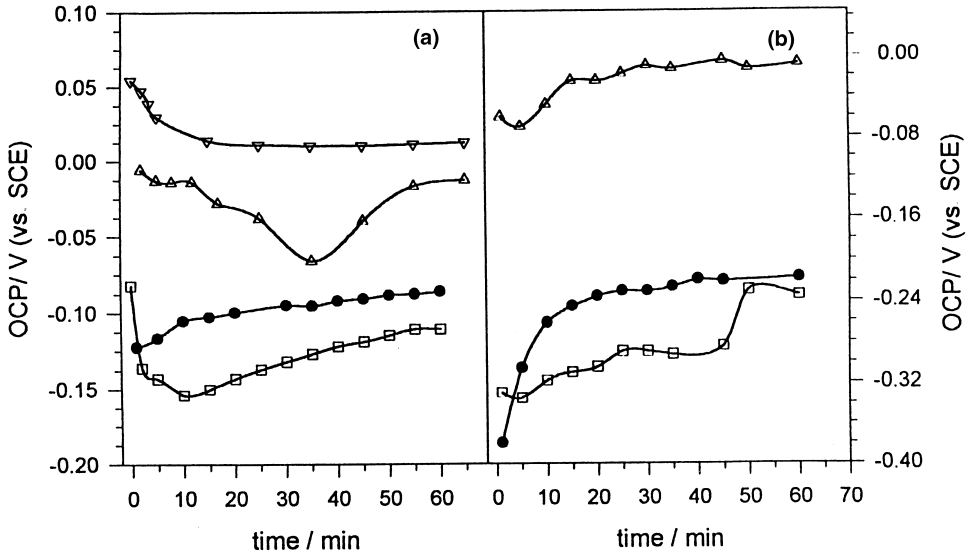

Fig. 3. OCP against time plot for (a) SS and (b) Ti in SCW saturated with O_2 or O_2/O_3 mixture: key for (a) (●) O_2; (□) O_2/O_3, $[O_3]$ = 0.15 ppm; (△) O_2/O_3, $[O_3]$ = 0.60 ppm; (▽) O_2/O_3, $[O_3]$ = 0.78 ppm; key for (b) (●) O_2; (□) O_2/O_3, $[O_3]$ = 0.18 ppm; (△) O_2/O_3; $[O_3]$ = 1.15 ppm.

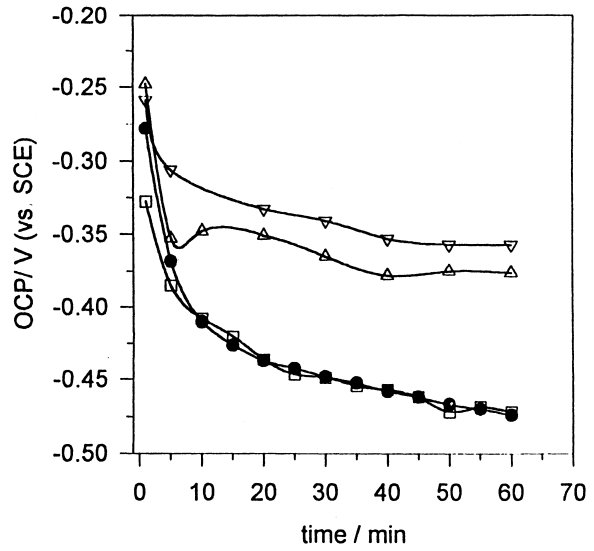

Fig. 5. OCP against time plot for mild steel in SCW saturated with: (●) O_2; (□) O_2/O_3, [O_3] = 0.15 ppm; (△) O_2/O_3, [O_3] = 0.38 ppm; (▽) O_2/O_3, [O_3] = 0.90 ppm.

The OCP evolution for copper and its alloys is shown in Figure 7. In oxygen saturated SCW (Figure 7(a)) the potential increased to reach a stable value. In the case of copper–nickel, a peak was formed before reaching this stable value. When the SCW was saturated with oxygen/ozone mixture, the OCP was unstable. There was an initial abrupt decrease followed by a potential increase. Again, the higher the ozone concentration, the higher the final OCP value.

To study the possible effect of ozone on the structure of passive layers formed on copper, cyclic potential scans were made at 0.020 V s^{-1} scan rate in SCW saturated with O_2 or O_2/O_3 mixtures. Voltammograms in SCW previously deaerated with nitrogen were also made (Figure 8). The anodic scan between −1.00 V and 0.20 V showed a peak (Ia) related to the formation of Cu(I) species. At higher potentials an increase in current was detected (IIa). This current increase has been attributed to Cu(II) dissolution [10]. The cathodic scan showed two peaks: Ic and IIc. In the deaerated solution, peak IIc was split in two peaks: IIc and II′c. In the presence of O_2/O_3 mixture the dissolution process occurred at higher potentials and the height of peak Ic changed.

To assess the effect of pH on the electrochemical behaviour of copper, cyclic potential scans were run in SCW added with a phosphate–borate buffer (pH 8) (Figure 9). Significant changes in the electrochemical behaviour of copper with respect to that shown in Figure 8 can be noticed. Only peak Ia could be seen in the anodic scan up to 0.2 V. The current increase associated with the dissolution process was not noticeable in this potential range. Higher anodic and cathodic

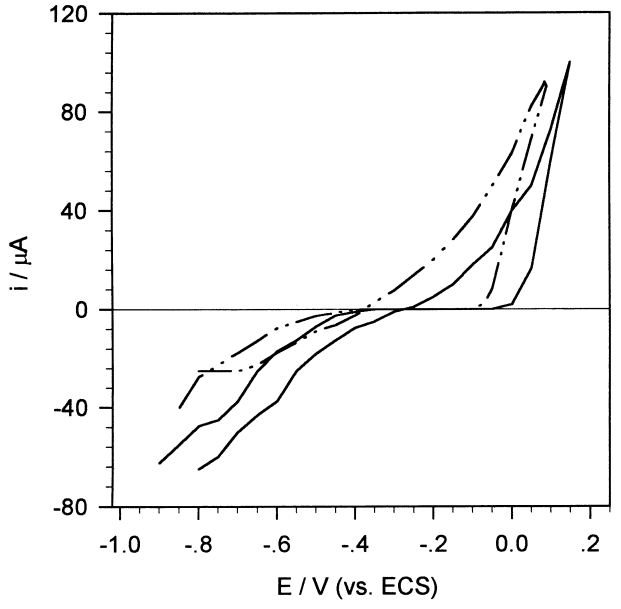

Fig. 6. Cyclic voltammograms for mild steel at 0.001 V s^{-1} in SCW saturated with O_2 or O_2/O_3 mixture. Key: (——) O_2 and (— · ·) O_3 = 0.6 ppm.

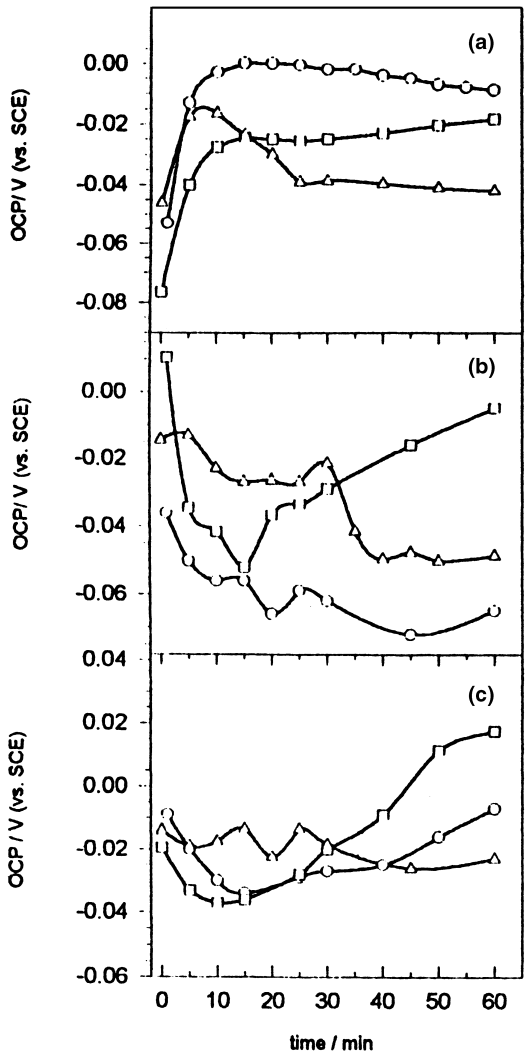

Fig. 7. OCP against time plot for copper (○); copper–nickel 70:30 (△) and aluminium brass (□) in SCW saturated with: (a) O_2; (b) O_2/O_3 mixture [O_3] = 0.12 ppm; (c) O_2/O_3 mixture [O_3] = 0.9 ppm.

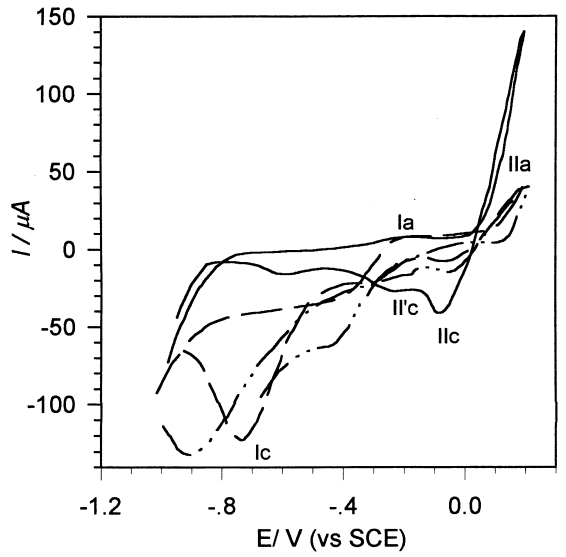

Fig. 8. Cyclic voltammograms for copper at 0.020 V s^{-1} in SCW saturated with: N_2; O_2 or O_2/O_3 mixture. Key: (— —) O_2, (—· -) $O_3 = 0.8$ ppm and (——) N_2.

currents were observed in the presence of O_2 and O_2/O_3 mixtures.

Figure 10(a) and (b) show the cyclic polarization curves for 70:30 copper–nickel and aluminium brass at 0.001 V s^{-1}. Similar E_b values were obtained for 70:30 copper–nickel in the presence and in the absence of ozone (Figure 10(a)). Conversely, in the case of aluminium brass, lower E_b values were observed when ozone was present (Figure 10(b)). A comparison between the OCP values for all the metals tested, measured after a 60 min contact time, and the E_b, measured through voltamperometric scans, is made in Table 4. An increase in the OCP values for the higher ozone concentrations is observed in all cases.

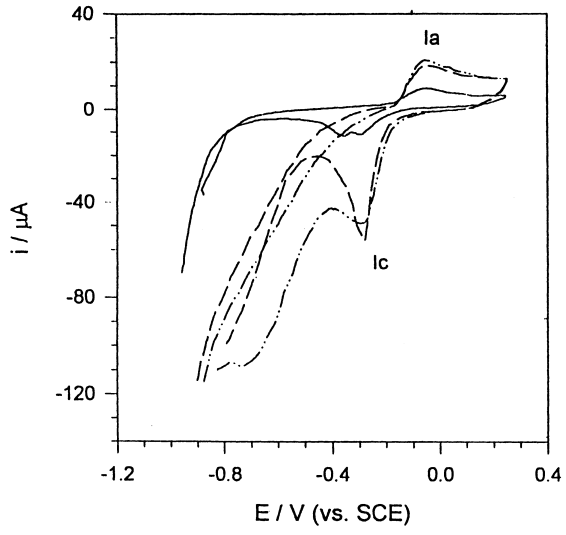

Fig. 9. Cyclic voltammograms for copper at 0.020 V s^{-1} in SCW + phosphate borate buffer (pH 8.5) saturated with: N_2; O_2 or O_2/O_3 mixture. Key: (——) N_2, (— —) O_2 and (— ·· —) $O_3 = 0.8$ ppm.

Figure 11 shows that the OCP against log time for titanium increases linearly in SCW with different ozone concentrations. This linear relationship is often associated to the formation of a barrier film [11].

4. Discussion

The metals tested can be divided in two groups: (i) metals whose passive behaviour in SCW is not affected by ozone (namely stainless steel and titanium); and (ii) metals which are susceptible to corrosion in the presence of ozone (i.e. carbon steel, copper and its alloys).

4.1. *Stainless steel and titanium*

The passive behaviour of stainless steel and titanium in SCW was not affected by ozone. However, the different OCP evolution pattern in the presence of O_2 or O_2/O_3 mixtures indicates that the characteristics of the protective film varied according to the oxidizing power of each solution.

In both metals, the potential increase in the presence of O_2 indicates that the formation of a barrier film starts immediately after the immersion of the electrode in the solution. However, in the presence of ozone there was an initial decrease in the OCP that may be associated to dissolution processes which take place before the formation of a barrier film. At the highest ozone concentration assayed, the OCP decrease was higher for stainless steel. A competition between the dissolution process and the passive film formation may exist, being the passivation process faster at the highest ozone concentration. Moreover, the initial OCP decrease was not observed under these conditions.

The difference between the OCP of stainless steel in O_2 and O_2/O_3 solutions (Figure 3) was similar to the difference between redox potential (Figure 2) for both solutions. Even for the small O_3/O_2 relationships assayed (5% maximum) the cathodic reaction of O_3 reduction is predominant over other possible reactions (i.e., oxygen reduction) [12].

It was suggested that the redox potential could be used as an indication of the ozone concentration for concentrations below 0.1 ppm [4]. However, the present results show that special care must be taken in relation to changes that may be produced in redox potential by the electrolyte composition as well as by different contact times.

OCP measurements can be useful to detect changes in the spontaneous evolution of barrier films such as those related to the thickness of the oxide layer and the alteration of the passivation mechanisms [11].

The ennoblement of OCP associated to the formation of a barrier film on the metal surface usually follows a logarithmic behaviour. Figure 11 shows that the OCP against log time for titanium increases linearly in SCW with different ozone concentrations. This effect was

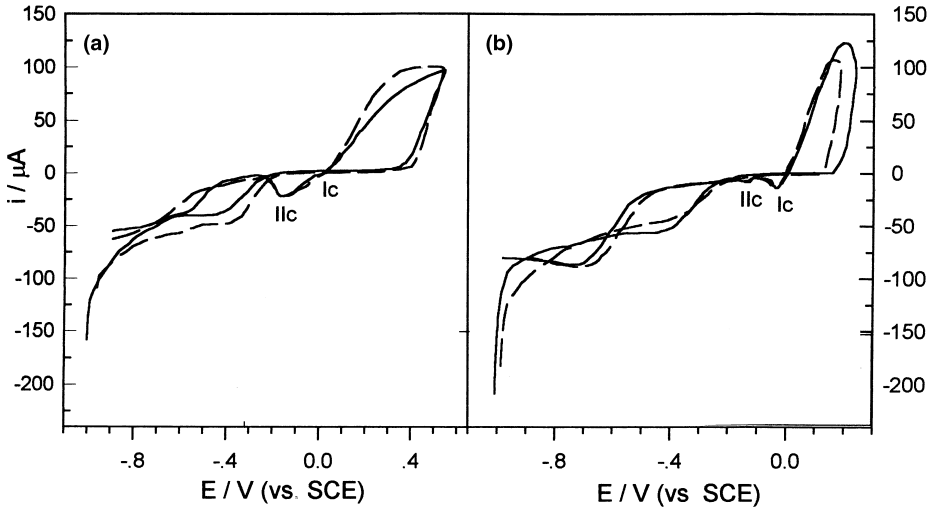

Fig. 10. Cyclic voltammograms for (a) copper nickel and (b) aluminium brass at 0.001 V s^{-1} in SCW saturated with O_2 or O_2/O_3 mixture. Key for (a): (— —) $O_3 = 0.7$ ppm and (——) O_2; key for (b): (——) O_2 and (— —) $O_3 = 0.13$ ppm.

attributed to the thickening of the barrier film. This barrier film grows in two dimensions and then in three dimensions through a solid state mechanism [12]. A change in the rate of potential increase could indicate: (i) growth in two dimension and then in three dimensions; (ii) variations in film properties; and/or (iii) the contribution of other processes like anion adsorption on the film.

When the diffusion of anions is restricted and the film grows according to a dissolution-precipitation process the OCP decreases initially [12]. In the presence of ozone, the higher dissolution of the metal requires the diffusion of ions from the metal to the solution through the layer of corrosion products.

The stainless steel passive behaviour is not affected by ozone. However, according to Figure 4 passivity is reached at lower potentials when ozone is present. Besides, higher oxidation rates in the presence of ozone with respect to oxygen may lead to the accumulation of cations at the interface.

Table 4. OCP values after 60 min in SCW saturated with O_2/O_3 mixture and E_b values

Metal	$[O_3]$ /ppm	OCP /V	$[O_3]$ /ppm	E_b /V
Ti grade 1	0.18	−0.235	1	not detected
	1.15	−0.008		up to 0.5 V
Stainless steel	0.15	−0.111	0.3	not detected
	0.63	−0.015		up to 0.5 V
	0.78	0.012		
Carbon steel	0.38	−0.376	0.60	−0.070
	0.90	−0.357		
Cu:Ni	0.12	−0.007	0.7	0.400
	0.9	−0.023		
Aluminium brass	0.12	–	0.13	0.150
	0.9	0.0175	0.8	0.170

4.2. *Carbon steel, copper and its alloys*

4.2.1. *Carbon steel*

The OCP of carbon steel decreases towards more active potentials due to the polarizing current supplied by the pits, which were detected by microscopic observations at the end of each experiment.

It has been reported [13] that E_b values of carbon steel obtained in deaerated SWC were more anodic than those obtained in O_2/O_3 mixtures. This result was interpreted as a passivating action of ozone. However, the effect of oxygen was not taken into account by the authors. Our results show that, even though E_b values obtained in O_2/O_3 saturated solutions were higher than those obtained in deaerated solutions, they were lower

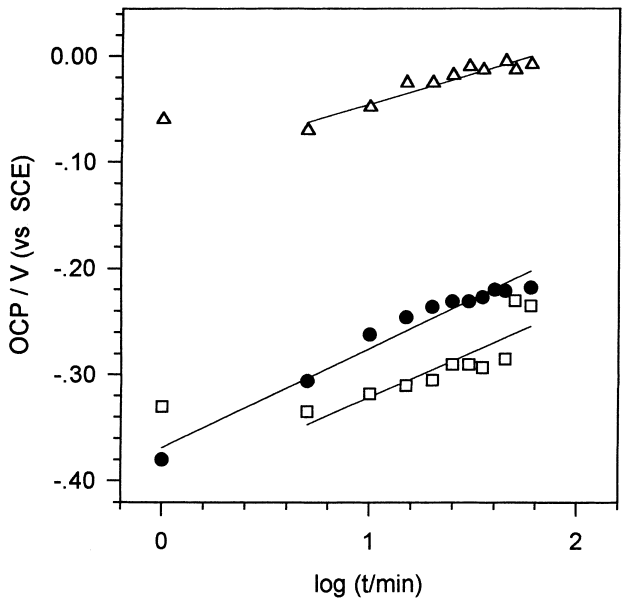

Fig. 11. OCP against log time plot for Ti in SCW saturated with O_2 or O_2/O_3 mixture: (●) O_2; (□) O_2/O_3, $[O_3] = 0.18$ ppm; (△) O_2/O_3, $[O_3] = 1.15$ ppm.

than those obtained in O_2 solutions. Besides, carbon steel E_r values in the presence of ozone were lower than those obtained in oxygen saturated solutions. This result suggests that in the presence of ozone pits remained active in a more extended potential range because the repassivation process is hindered by ozone.

4.2.2. *Copper and alloys*

For these metals, the OCP evolution in ozone containing solutions differs from that observed in the absence of ozone. The OCP decreases to reach a minimum value and then increases in the ozonated solution. In the absence of ozone the OCP increases before becoming stable. The potential increase may be associated with the growth of a duplex oxide structure on the surface [15]. Conversely, the OCP decrease can be related with an increase in the anodic reaction/cathodic reaction surface ratio which results in an increase in the dissolution rate [16]. This effect was not observed in buffered solutions, indicating a marked influence of pH and probably anion adsorption in the process [17].

Our data can be interpreted as the result of a competition between the cuprous oxide formation and dissolution related processes. Elipsometric measurements revealed changes in the optical parameters related to the oxide thickness as well as to the formation of hydrated layers in the presence of ozone [17]. The amount and the distribution of the charge involved in the potentiodynamic reduction process differed markedly if solutions were saturated with N_2, O_2 or O_2/O_3. In each case, the direction of the reaction will depend on the dissolved ozone concentration, the oxidizing characteristics of the solution, the amount of previously formed oxides and the contact time.

The passivity breakdown of copper and its alloys occurs at more noble potentials in the presence of oxygen or oxygen/ozone mixtures than in the presence of nitrogen. In the former case the height of peaks IIc associated to the reduction of oxygenated species decreases while the current of peak Ic increases (Figure 8). When oxygen/ozone mixtures were used, the peak Ic increased in height and was shifted in the cathodic direction. These results showed the electrochemical behaviour of copper changes according to the oxidizing characteristics of the solution. Copper behaviour is strongly influenced by the pH. The dissolution of copper produces a decrease in the interfacial pH [15, 17]. In buffered solutions, the formation of Cu(I) occurs up to 0.20 V and the formation of Cu(II) is hindered [10]. In nonbuffered solutions, the pH drop prevents the precipitation of Cu_2O, favouring the oxidation of Cu(I) to Cu(II).

The polarization curves of copper–nickel and aluminium brass show that both alloys have a wider passive region than pure copper due to the presence of the alloying elements. The beginning and the end of the passive region are similar in SCW either with O_2 or O_2/O_3. However, the E_b of aluminium brass in the presence of ozone is low, probably due to the easier dissolution of the less noble alloying element (Zn) [18]. OCP values for aluminium brass are close to the E_b value showing a hazardous situation at high ozone concentrations.

5. Conclusions

(i) OCP against time measurements can be useful for detecting changes in the spontaneous formation of oxide layers. All the metals tested, except carbon steel, showed an OCP increase up to stable value in the presence of pure oxygen. In contrast, SCW saturated with O_2/O_3 mixtures initially showed a decrease in the OCP, probably associated to a dissolution processes. The passivity of titanium and stainless steel was not affected by ozone. A linear OCP against log time relationship was found for titanium, suggesting the growth of a barrier film in both O_2 and O_2/O_3 solutions.

(ii) The high OCP values measured in ozone containing solutions can be associated to opposite conditions: (a) a passive state (OCP is far from E_b) or (b) a high susceptibility to localized attack (OCP reaches a value close to E_b).

(iii) Mild steel did not passivate in SCW either with O_2 or O_2/O_3 in the solution. Ozone facilitates the breakdown of passivity and makes the repassivation difficult.

(iv) Ozone enhances the dissolution of Cu_2O and the formation of Cu(II) species. The net result of the competition between these processes will depend on (i) the nature of the electrode; (ii) the ozone concentration; (iii) the composition, oxidizing characteristics and pH of the solution, (iv) contact times used. Less noble alloying elements of aluminium brass render the alloy more susceptible to dissolution in the presence of ozone.

(v) A discontinuous treatment with ozone may cause changes and instability in the oxidation products enhancing the corrosion tendency.

Acknowledgements

This work was supported by the University of La Plata, the Consejo Nacional de Investigaciones Científicas y Técnicas (CONICET) and the Agencia Nacional de Promoción Científica y Tecnológica of Argentina.

References

1. S. Hettiarachchi, Corrosion '91, Paper 206 (edited by NACE International), Houston, TX (1991).
2. E.L. Domingue, R.L. Tyndall, W.R. Mayberry and O.C. Pancorbo, *Appl. & Environ. Microbiol.* **54** (1988) 741.
3. O. Leitzke and G. Greiner, *Vom Wasser* **67** (1986) 49.
4. R.G. Rice and J.F. Wilkes, Corrosion '91, Paper 205 (edited by NACE International), Houston, TX (1991).
5. B. Yang, D.A. Johnson and S.H. Shim, *Corrosion* **49** (1993) 499.

6. M. Matsudaira, M. Suzuki and Y. Sato, *Mater. Perform.* **21** (1981) 55.
7. R.J. Strittmatter, B. Yang and D.A. Johnson, Corrosion '92, Paper 347 (edited by NACE International), Houston, TX (1992).
8. H.A. Videla, M.R. Viera, P.S. Guiamet, M.F.L de Mele and J.C. Staibano Alais, Corrosion '95, Paper 199 (edited by NACE International), Houston, TX (1995).
9. H. Bader and J. Hoigne, *Wat. Res.* **15** (1981) 449.
10. M. Pérez Sánchez, M. Barrera, S. González, R.M. Souto, R.C. Salvarezza and A.J. Arvia, *Electrochim. Acta* **35** (1990) 1337.
11. A.G. Gad-Allah and H.A. Abd El-Rahman, *Corrosion* **43** (1987) 698.
12. H.H. Lu and D.J. Duquette, *Corrosion* **46** (1990) 843.
13. B.E. Brown, H.H. Lu and D.J. Duquette, *Corrosion* **48** (1992) 970.
14. H.A. Videla, M.R. Viera, P.S. Guiamet, S. Gómez de Saravia and C.C. Gaylarde, Corrosion '96, Paper 286 (edited by NACE International), Houston, TX (1996).
15. J.O. Zerbino and M.F.L. de Mele, *J. Appl. Electrochem.* **27** (1997) 335.
16. L. Admiraal, F.P. Ijsseling, B.H. Kolster and J. van der Veer, *Br. Corros. J.* **21** (1986) 33.
17. M.F.L. de Mele, M.R. Viera and J.O. Zerbino, *J. Appl. Electrochem.* **27** (1997) 396.
18. Z. Xia and Z. Szklarska-Smialowska, *Corrosion* **46** (1990) 85.